Article:
Qiao, P, Harbottle, D, Tchoukov, P et al. (4 more authors) (2017) Fractionation of Asphaltenes in Understanding Their Role in Petroleum Emulsion Stability and Fouling. Energy & Fuels, 31 (4). pp. 3330-3337. ISSN 0887-0624

https://doi.org/10.1021/acs.energyfuels.6b02401

Fractionation of Asphaltenes in Understanding Their Role in Petroleum Emulsion Stability and Fouling: A Critical Review

Peiqi Qiao[1], David Harbottle[2], Plamen Tchoukov[1], Jacob Masliyah[1], Johan Sjoblom[3], Qingxia Liu[1] and Zhenghe Xu[1]

[1]Department of Chemical and Materials Engineering, University of Alberta, Canada

[2]School of Chemical and Process Engineering, University of Leeds, UK

[3]Ugelstad Laboratory, Norwegian University of Science and Technology, 7491 Trondheim, Norway

ABSTRACT

SARA fractionation separates the oil into fractions of saturates (S), aromatics (A), resins (R), and asphaltenes (A) based on the differences in their polarizability and polarity. Defined as a solubility class, asphaltenes are normally considered as a menace in the petroleum industry mainly due to their problematic precipitation and adsorption at oil water and oil-solid interfaces. As a broad range of molecules fall within the group of asphaltenes with distinct sizes and structures, considering the asphaltenes as a whole was noted to limit the deep understanding of governing mechanisms in asphaltene-induced problems. Extended-SARA (E-SARA) is being proposed as a concept of asphaltene fractionation according to their interfacial activities and adsorption characteristics, providing critical information to correlate specific functional groups with certain characteristics of asphaltene aggregation, precipitation and adsorption. Such knowledge obtained is essential to addressing asphaltene-related problems by targeting specific subfractions of asphaltenes for selective removal.

1. INTRODUCTION

1.1 SARA

Derived from ancient fossilized organisms, petroleum crude oil is a complex organic mixture comprising of saturated and unsaturated hydrocarbons with small amounts of heteroatoms (N, O, and S) and metallic constituents.[1] The characterization of crude oil is critical not only to oil processing from upstream reservoir exploration to downstream refining design, but also for prediction and management of environmental exposure.[2] Due to the complex nature of crude oil, it is almost impossible to identify individual molecules present in it. Bulk properties of crude oils, such as density (or API gravity), viscosity and boiling point, are often measured to give a fast assessment of petroleum oil, in the context of various types of oil separation processes based on boiling point (distillation), solubility (precipitation) and chromatography (adsorption).[3] These physical properties are determined by chemical compositions and structures as well as molecular weights of the crude oil components.

SARA fractionation uses a combination of solubility and chromatographic separation, which separates the crude oil into fractions of saturates (S), aromatics (A), resins (R) and asphaltenes (A) according to their polarizability and polarity (Figure 1).[4–6] In SARA fractionation, asphaltenes are first precipitated using n-alkanes, such as n-pentane or n-heptane.[4,7] After removal of asphaltenes, the remaining SARA fractions are sequentially obtained by eluting the remaining components, collectively called maltenes. Maltenes are adsorbed onto a chromatographic column using various solvents of particular polarity. Saturates consisting mainly of non-polar linear, branched and cyclic alkanes are removed by flushing the maltenes with n-alkanes through the column, with all other remaining components adsorbed onto the column.[4,8] The aromatic fraction is separated (washed off) from the adsorbent in the column using aromatic solvent such as benzene, and resins are eluted from the column with polar solvent such as methanol and chloroform. Aromatics contain compounds with one or more aromatic rings in which heteroatoms are normally embedded.[4,9] Resins and asphaltenes are operationally defined as two solubility classes containing various types of polar components with aromatic rings.[4,10,11] Resins are soluble in n-heptane and n-pentane, but insoluble in liquid propane; whereas asphaltenes are

insoluble in n-alkanes, but soluble in toluene. The polarizability of all SARA fractions increases from saturates to asphaltenes.

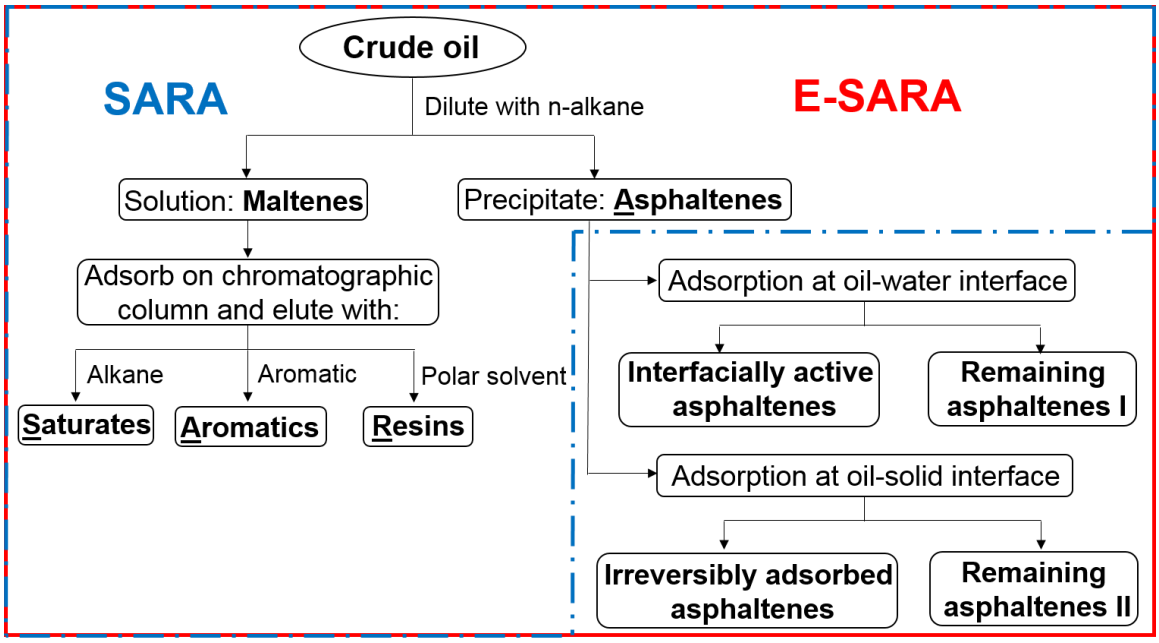

Figure 1. Comparison of conventional SARA and extended-SARA (E-SARA) analysis.

SARA analysis does not provide sharp boundaries between various fractions. The yield of each of the fractions in chromatography depends on the eluting solvent and adsorbent (column materials) used. For example, the mass fraction of asphaltenes recovered using n-heptane is lower than that using n-pentane, due to their higher solubility in n-heptane than in n-pentane.[12] Moreover, the results of SARA analysis using different techniques and/or from different laboratories can vary greatly.[13,14] Despite these ambiguities, SARA analysis has become a widespread characterization method of crude oil. SARA analysis results have successfully guided the processing and refining paths of crudes based on the quantity of asphaltenes in crudes. Asphaltenes precipitate when the temperature/pressure changes, or the oil loses its light components, or is mixed with a paraffinic solvent, or is blended with a paraffinic crude.[4,15] Such precipitation may lead to the deposition of asphaltenes in production wells and pipelines (Figure 2a), resulting in the flow restriction, or even bringing oil production to a halt.[4,15–20] In addition, asphaltenes play a significant role in the stabilization of water-in-oil (W/O) emulsions[21–26] (Figure 2b) which lead to severe

corrosion problems in production and transportation due to the dissolved salts and entrained fine solids carried by emulsified water droplets.[4] Moreover, an oil with high content of asphaltenes tends to form coke when heated, which is highly detrimental to heat exchangers and catalyst beds in upgrading and refining.[4,19,27,28] Because of its simplicity, SARA analysis is a reasonable first step in characterizing oils, providing warning for potential asphaltene-related losses suffered by oil industry.

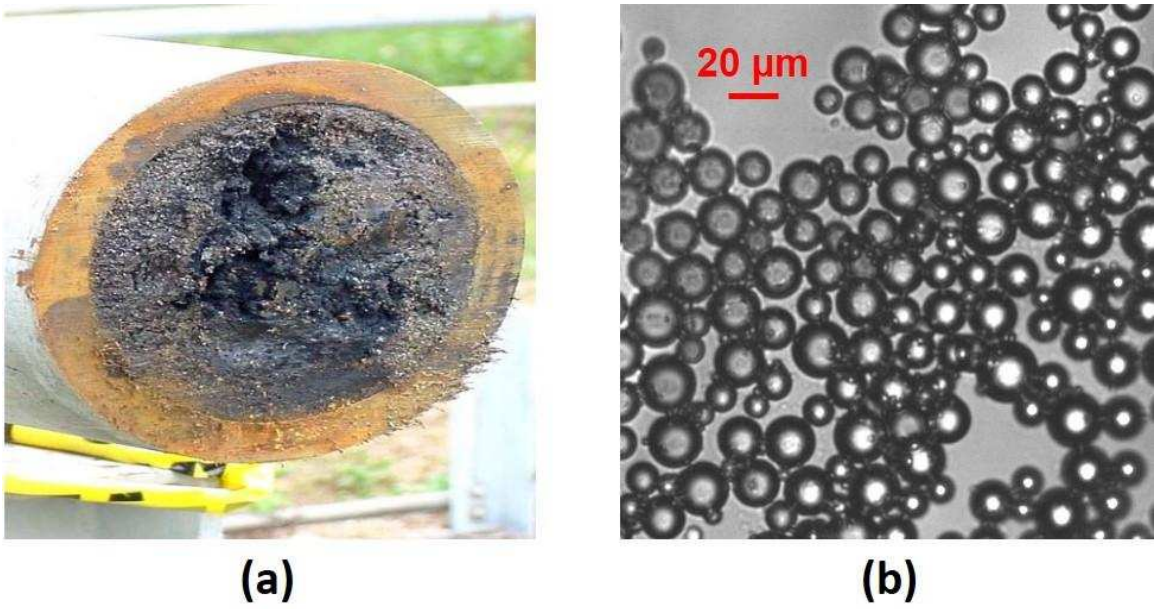

Figure 2. (a) The pipeline was plugged with asphaltenes. Reprinted with permission from Torres et al.[20] Copyright 2005 Society of Petroleum Engineers. (b) Microscope image of a typical W/O emulsion stabilized by asphaltenes, prepared by homogenizing 20 mL of DI water in 100 mL of 10 g/L asphaltene-in-toluene solution at 30000 rpm for 5 min.

1.2 Asphaltenes

Asphaltenes are not a specific family of chemicals with a common functional group. Individual molecules in the spectra of asphaltenes may have distinct chemical structures. Until very recently, the average molecular mass values of asphaltenes were reported to span six orders of magnitude from less than one thousand up to tens of millions daltons.[29] However, this has now been refined and the well accepted molecular weights of asphaltenes are between 500 Da and 1000 Da with an average molecular weight of 750 Da,

depending on the source of oil.[30] Asphaltenes consist mainly of carbon, hydrogen, nitrogen, oxygen and sulfur, with trace amounts of metals such as vanadium, nickel and iron. While the elemental composition of asphaltenes is well-recognized, there had been long-standing debate as to whether the asphaltene compounds comprise of one polycyclic aromatic hydrocarbon (PAH) core with peripheral alkyl and naphthenic groups, or multiple cross-linked PAHs, known as the island and archipelago model of asphaltenes, respectively. Recent work by Schuler et al. indicated that asphaltenes are dominated by one large fused aromatic hydrocarbon ring with peripheral alkyl substituents. Combining atomic force microscopy (AFM) with scanning tunneling microscopy (STM), the authors identified island structures of more than one hundred asphaltene molecules.[31]

Aggregation behavior of asphaltenes has been another subject of controversy that receives substantial attention. Asphaltenes are known for their inevitable self-aggregation, even in good solvents such as toluene.[32,33] The aggregation of asphaltenes is enhanced with decreasing aromaticity of the solvent.[34,35] Dickie and Yen[36] and later Mullins[37] proposed a stepwise aggregation model of asphaltenes, known as the Yen-Mullins model,[38] including formation of asphaltene nanoaggregates and clusters (Figure 3). According to Yen-Mullins model, asphaltene molecules are dominated by island architecture with most probable molecular weight of ~750 Da, as supported by recent mass spectral analysis.[39–41] Approximately six asphaltene molecules form a nanoaggregate via π-π stacking of their PAH cores. The asphaltene nanoaggregates can further associate to form clusters with aggregation numbers of approximately eight. The aliphatic side chains around PAH cores were believed to impose a steric repulsion that limits the aggregation number. The sizes of the asphaltene nanoaggregates and clusters were estimated to be around 2 nm and 5 nm, respectively. More recent work by Gray et al. proposed the formation of complex macro-molecular aggregates of asphaltenes through three-dimensional "supramolecular assembly model".[42] These authors suggested that asphaltene aggregation is a cumulative effect of various intermolecular interactions, including acid-base interactions, hydrogen bonding, metal coordination complexes, hydrophobic pockets, aromatic π-π stacking, etc. Such multi-cooperative association would explain the porous structures of asphaltene aggregates

with a range of sizes and shapes, exhibiting polydispersity in population. Molecular dynamics simulation studies confirmed that asphaltene aggregation results in the formation of complex structures both in the bulk and at the oil-water interface.[43–46] The strong self-aggregation of asphaltenes facilitates the adsorption of asphaltenes at oil-water interfaces, which is crucial for the stabilization of oil-water petroleum emulsions, and also the adsorption of asphaltenes onto mineral and metallic surfaces, which leads to plugging and fouling through entire oil production chains.

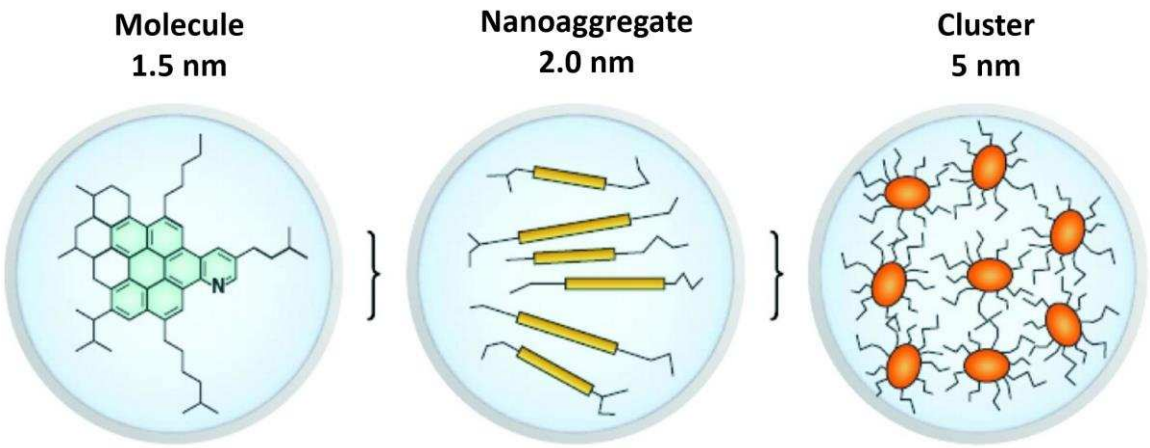

Figure 3. Yen−Mullins model to describe asphaltene aggregation. Reprinted with permission from Mullins et al.[38] Copyright 2010 American Chemical Society.

1.3 Asphaltene adsorption

The interfacial and surface activity of asphaltenes has long been studied due to the processing challenges that are encountered once asphaltenes begin to accumulate at oil-water and oil-solid interfaces. Earlier studies have shown that a water droplet aged in a diluted crude oil or asphaltene solution experienced crumpling upon volume reduction, which was attributed to the irreversible asphaltene adsorption at the oil-water interface.[35,47,48] Following the time-dependent adsorption of asphaltenes, Freer and Radke[49] conducted measurement after replacing the existing solutions with pure solvent for a few times, and reported only a marginal increase in the oil-water interfacial tension (~1.5 mN/m), confirming the irreversible adsorption of most asphaltene molecules. After the washing, the frequency-dependent responses of interfacial dilatational moduli (storage

(E') and loss (E") moduli) of the asphaltene film were in excellent agreement with the Maxwell model for irreversibly adsorbed species. When studying the surface pressure isotherms of asphaltene films, Yarranton et al.[50] showed a lower compressibility with increasing aging time of the films. The presence (formation) of solid-like (elastic dominant) asphaltene films at the oil-water interface has been shown to significantly hinder the coalescence of two contacting water droplets, as such that when two droplets interact and undergo significant compression, they continue to remain stable without coalescence.[48,51]

The correlation between interfacial dilatational elasticity and overall emulsion stability has been qualitatively proven by several researchers,[49,50,52–56] although there is clear disagreement at high asphaltene concentrations where emulsion stability increases and E' decreases. The discrepancy between the interfacial rheology and emulsion stability is believed to be associated with a change in the interfacial layer structure, transitioning from a compact and rigid monolayer, to a collapsed interfacial layer dominated by three-dimensional structures.[55] More recently, the shear rheological response (storage (G') and loss (G") moduli) of asphaltene films has been studied following the introduction of interfacial geometries.[54,51,57] With a biconical bob geometry, Spiecker and Kilpatrick investigated the evolution of the shear elasticity (G') for asphaltene films.[54,57] It was shown that stronger asphaltene films of higher elasticity and yield stress are more favored under conditions such as high asphaltene concentration, low solvent aromaticity and asphaltenes of high polarity. Using double wall ring geometry, Harbottle et al. showed that asphaltene films exhibit time-dependent viscoelasticity, transitioning from a liquid-like film (G">G') at short aging times to a solid-like film (G'>G") at longer aging times.[51] The transition in rheological response was found to correspond to a transition in the observed droplet stability that the droplets coalesce readily within seconds in the liquid-like state, and they remain stable without coalescence in the solid-like state. The contributing factor to the enhanced droplet stability is the development of a yield stress in the asphaltene network, which must be overcome to initiate the mobility within asphaltene films and subsequent droplet coalescence. The authors directly compared the shear and dilatational rheological responses, demonstrating that shear is the dominate mode of interfacial deformation due to

the high energy cost associated with dilatational deformation. The importance of yield stress has also been underlined by thin-liquid film drainage experiments which use photo-interferometry to accurately measure the thickness of draining asphaltene films.[58] Following interfacial aging, the drainage kinetics was significantly retarded and thick asphaltene films with extended lifetimes were measured. The deviation between experiment and theory (Stefan-Reynolds equation) was addressed by accounting for the liquid film yield stress, i.e. resisting force as two asphaltene films interact.

The interaction of asphaltenes with solid surfaces has also received significant scientific attention due to its importance in preventing pipeline blockages and wettability modifications of fine solids. The oil wettability of fine clays increases with increasing asphaltene adsorption, increasing the potential for clays to stabilize W/O emulsions.[19,26,59] A range of experimental techniques have been adopted to study the adsorption of asphaltenes onto several different substrates including silica,[60–62] alumina,[61,62] iron oxide,[63] gold,[43,51,60,64–67] stainless steel,[66] glass[68], and clay minerals.[69–78] Using quartz crystal microbalance with dissipation (QCM-D), asphaltene adsorption and film formation have been studied in real time.[51,60,61,64–66] X-ray photoelectron spectroscopy (XPS),[65,75] X-ray diffraction (XRD),[72,74,75] small-angle X-ray scattering (SAXS),[74] Fourier transform infrared spectroscopy (FTIR)[71,72,74] and Fourier transform ion cyclotron resonance mass spectrometry (FT-ICR MS)[73] have been applied to characterize the surface modification by asphaltene adsorption. It is however not straightforward to compare the results from different adsorption studies since asphaltene adsorption is a complex process affected by many aspects such as source of asphaltenes, type of solvents (quality and composition), moisture content of solvents, flow condition, temperature, etc. The adsorption process often follows a Langmuir-type isotherm, although the mechanism for film formation and factors which contribute to monolayer and multi-layer films continue to be debated.[51,60,64–67,70,75] The detailed discussion of adsorption "isotherms" is outside the scope of this article. Needless to say, adsorbed asphaltenes have been shown to be very stable. Removal of adsorbed asphaltenes by solvent washing has been proven mostly unsuccessful, with only partial removal reported for aggressive cleaning strategies using solvent such as toluene,

benzene, chloroform and acetone.[60,69,78,79] The irreversibility of asphaltene adsorption is a big problem that can eventually lead to pipeline blockage and equipment fouling.

2. EXTENDED-SARA (E-SARA)

Asphaltenes are defined by solubility rather than any analyzed chemical properties. Despite its simplicity, such generalized definition of asphaltenes has often limited our knowledge regarding the asphaltene-induced problems in crude oil processing. It was reported that rather than whole asphaltenes, only a subfraction of asphaltenes is more likely the real contributor to the stabilization of W/O emulsions.[26,80–86] The asphaltenes adsorbed onto clays have also been found to be different in composition from whole asphaltenes.[70,75–77] Therefore, it is important to find ways to extract and study these particular species from asphaltenes, which are mainly responsible for the relevant issues of interest. The fractionation of asphaltenes allows the investigation of these asphaltene subfractions thereby providing necessary information to improve our understanding of the governing mechanisms and develop efficient mitigating approaches to the related problems. Most existing work on the asphaltene fractionation are based on their solubility by precipitating different subfractions of asphaltenes using a mixture of aromatic solvent and aliphatic solvent with varying ratios.[25,87,88] However, it is more instructive to fractionate asphaltene molecules according to their problematic properties of research interest. Here, we introduce a new concept of extended-SARA (E-SARA) (Figure 1), the fractionation of asphaltenes based on their adsorption at oil-water and oil-solid interfaces. Through the studies of resulting asphaltene subfractions, E-SARA enables the identification of key functional groups which govern asphaltene adsorption at oil-solid interface and partition at oil-water interface, thus providing a greater understanding of the molecular mechanisms of observed challenges caused by asphaltene subfractions isolated by E-SARA analysis. With such approach, new routes to mitigate asphaltenes stabilizing oil-water emulsions, and adsorbing onto solid surfaces (flow assurance and fouling) can be sought.

2.1 Fractionation of asphaltenes based on asphaltene adsorption at oil-water interface

One of the major problems encountered in crude or heavy oil production is the formation of stable W/O emulsions. Resolution of these emulsions and water removal from oil feed to upgrading facilities is an important step in petroleum industry. A great deal of research was focused on understanding the stabilization mechanisms of W/O emulsions.[21–26] It was identified that asphaltenes play a key role in the emulsion stabilization; however, the exact mechanism is not entirely clear. As it was pointed out by Czarnecki et al.[83,84], the understanding that asphaltenes stabilize the emulsions in way similar to surfactants by lowering interfacial tension and giving rise of surface forces to prevent droplet coalescence is discounting the facts that asphaltenes as a whole do not have amphiphilic character and their structures are dominated by hydrophobic groups with few polar functionalities. These authors suggested that in fact only a small subfraction of asphaltenes is responsible for W/O emulsion stabilization, and blaming the asphaltenes as a whole is detrimental for the deep understanding of the related mechanisms.

Therefore, it is important to isolate and characterize interfacial active components of asphaltenes irreversibly accumulated at the oil-water interface. Wu developed an effective method to collect the interfacial materials (IM) of bitumen which adsorb at the surfaces of heavy water (D_2O) droplets dispersed in the W/O emulsion.[81] In this method, D_2O was mixed with heptol (a mixture of heptane and toluene at 1:1 volume ratio)-diluted bitumen to form a stable W/O emulsion. Regular deionized (DI) water was then added in the emulsion, followed by the centrifugation of the resulting mixture. After the centrifugation, the emulsified heavy water droplets containing IM passed through the oil-water interface and then DI water layer, finally settled down to form a cake on the bottom of the vessel due to the density difference. The DI water layer acted as a barrier to reduce bitumen contamination on the surfaces of heavy water droplets. The IM of bitumen were recovered by drying the wet cake. Through the characterization using FT-ICR MS, Stanford et al. reported that sulfur- and oxygen-containing species were enriched in the IM obtained using Wu's heavy water method as compared to the parent bitumen.[82] Jarvis et al. isolated the IM of crude oils based their interactions with the immobilized water layers on the hydrated

silica surface.[89] The interactions of oil compounds with silica substrate were inhibited by water monolayers generated on the surface of silica gel. The mixture of hydrated silica gel and heptol-diluted crude oil was loaded on the column at the beginning of the isolation. After the removal of non-interacting oil components by flushing the column with heptol, the IM solution was obtained by eluting the column using methanol/toluene (10:25 v/v) solution followed by the extraction with dichloromethane to minimize silica contamination. The solvent of IM solution was then evaporated upon drying under N_2. The IM isolated using this wet silica technique showed similar chemical functionalities with those obtained by Wu's heavy water method. These isolation techniques provided valuable information of interfacially active components of crude oils. In this line of thinking, Yang et al. developed an original method to extract only the subfraction of asphaltenes which is really involved in the stabilization of W/O emulsions, i.e. the asphaltene species that irreversibly adsorbed at oil-water interface.[85,86]

2.1.1 Fractionation procedure

Yang et al. fractionated the asphaltenes based on their affinity to toluene-water interface.[85] The entire fractionation procedure is schematically represented in Figure 4. Pentane-extracted asphaltenes from Athabasca coker feed bitumen (Syncrude Canada, Ltd., Canada) were referred to as whole asphaltenes (WA) in this work. WA were first dissolved in toluene at a concentration of 10 g/L, followed by homogenizing the WA-in-toluene solution with 10% (v/v) water at 30,000 rpm for 5 min. The resulting emulsion was then left for 24 h for equilibration. Through the centrifugation (20,000 g), the cake of emulsified water droplets was separated from the continuous oil phase. No apparent coalescence or free water was observed during centrifugation. The asphaltenes remaining in the oil supernatant were named as remaining asphaltenes (RA). Water droplets were then washed with an excessive amount of clean toluene until a clear washing toluene was observed indicating the complete removal of entrapped asphaltene-in-toluene solution and asphaltene species loosely bound to the interface. After the evaporation of water in a vacuum oven at 60 °C, the asphaltenes which were adsorbed at the surfaces of water

droplets were isolated and named as interfacially active asphaltenes (IAA). The extracted IAA subfraction was estimated to be less than 2 wt% of WA.

2.1.2 Chemical compositions

IAA subfraction is heavier than RA according to the results of electrospray ionization mass spectrometry (ESI-MS).[86] The molecular weight distribution of IAA peaked within the range of 1,000-1,200 Da, while the average molecular weight of RA was centered at about 700-750 Da, which is in good agreement with recent asphaltene studies.[30] The elemental analysis showed similar carbon, hydrogen, nitrogen, and sulfur contents for two subfractions; however, the oxygen content of IAA (5.54 wt%) is three times higher than that of RA (1.68 wt%). Such higher oxygen content of IAA is linked to the presence of sulfoxide groups as indicated from FTIR spectra, in which IAA subfraction exhibited a pronounced peak at 1020 cm^{-1}. Further analysis was conducted using ^{1}H and ^{13}C nuclear magnetic resonance (NMR) spectroscopy. All carbon types present in the asphaltene samples were determined using an original method developed at CanmetENERGY,[90] which allows for calculation of average segment lengths of hydrocarbon chains, and average cluster sizes of aromatic and cycloparaffinic rings. Based on the data of above analysis, the authors proposed an average molecular representation for IAA and RA, respectively, as shown in Figure 5. On average, IAA molecules have lower aromatic content and higher paraffinic content than RA. No significant difference was observed between WA and RA, which is reasonable considering that RA subfraction comprises more than 98 wt% of WA.

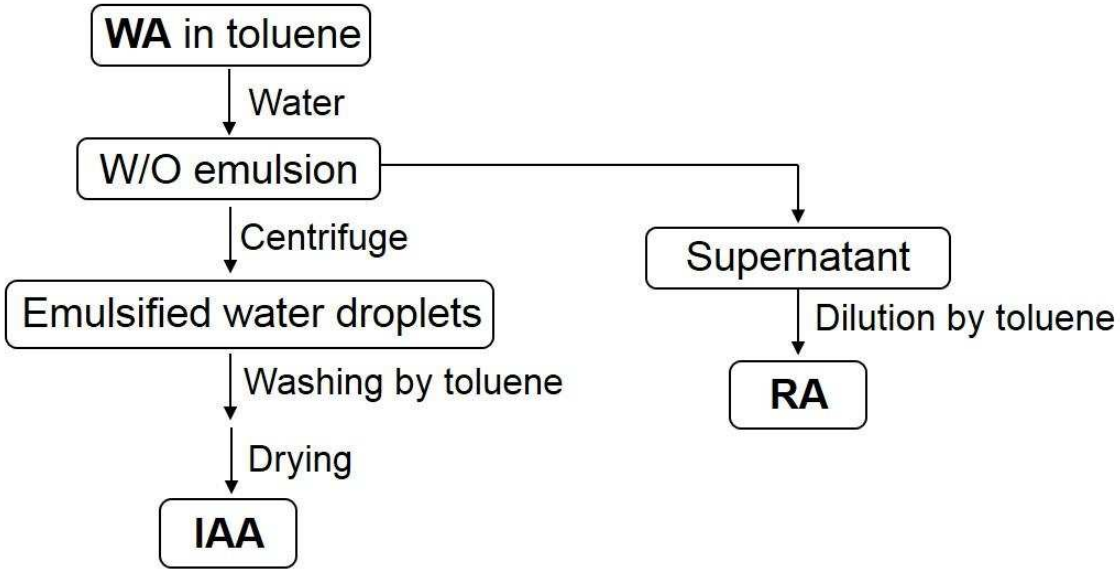

Figure 4. Procedure of asphaltene fractionation based on asphaltene adsorption at toluene-water interface. Adapted with permission from Yang et al.[85] Copyright 2014 American Chemical Society.

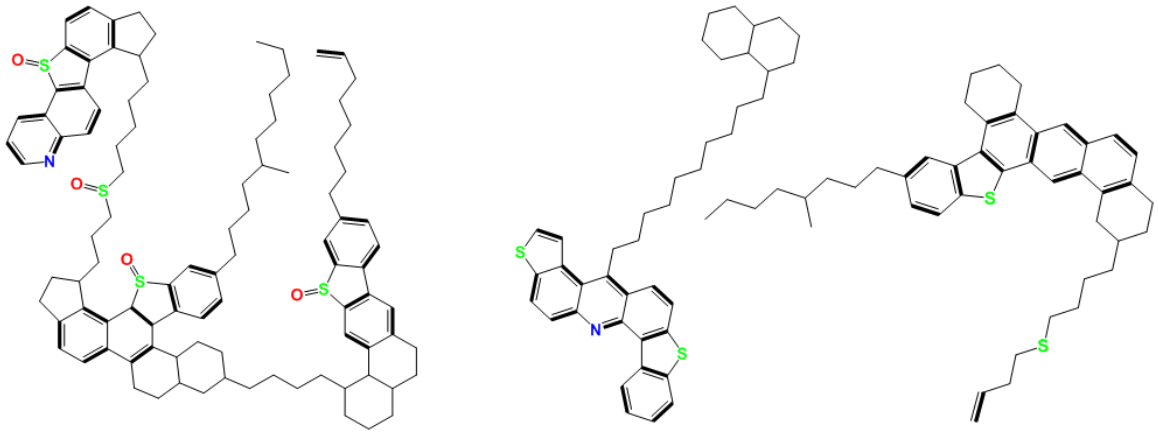

Figure 5. Molecular representations of IAA (left) and RA (right). Reprinted with permission from Yang et al.[86] Copyright 2015 American Chemical Society.

2.1.3 Interfacial properties

The interfacial tension of 0.1 g/L IAA-in-toluene solution against water was measured to be 24.0 mN/m after 1 h, in comparison with 29.5 mN/m for RA under the same conditions,

indicating IAA are more interfacially active than RA.[85] In addition, interfacial pressure-area isotherms showed that IAA formed a rigid layer with low compressibility, which is below 0.5 m/mN even at the initial stage of compression. In contrast, RA films were soft with high compressibility. Furthermore, the authors studied the relaxation process of the interfacial layers of IAA and RA by reducing the interfacial area until reaching the same target pressure of 20 mN/m. The relaxation of the interfacial pressure was then recorded for 20 min. The results indicated that the interfacial pressure decreases about 10% and 40% for IAA and RA, respectively. As compared to RA, the smaller reduction of interfacial pressure exhibited by IAA is interpreted as an indication of irreversible adsorption and less freedom for rearrangement of adsorbed molecules.

2.1.4 Emulsion stability and oil film properties

Despite the fact that IAA molecules represent only a small subfraction of WA, the bottle tests showed that the removal of IAA dramatically decreased the stability of W/O emulsion.[85] In addition, using thin liquid film technique, which was proven to be a useful tool for understanding the stabilization mechanisms of W/O emulsions, Yang et al. evaluated the stability of oil films formed by IAA-, RA-, and WA-in-toluene solutions. Through the direct studies of thin oil layers separating water phases, they found that IAA formed very stable films, which did not rupture for 20 min; however, the average lifetime for WA films and RA films is ~500 s and less than 20 s, respectively. Such data agrees well with emulsion stability results obtained from bottle tests. Microscopic images revealed that RA and IAA emulsion films have significantly different morphology and film thickness. The dark background of the RA film indicates that the film thickness is about 30-40 nm. RA films ruptured in less than 1 min, and no apparent aging effects were observed. In contrast to RA films, the IAA film was much thicker (above 100 nm) with a significant variation in the thickness inferred by the Newton fringes. These thick lenses indicate the formation of aggregates in the IAA film, which was not observed initially before 30 min aging. These films are similar to asphaltene-in-toluene films as reported by Tchoukov et al.[58] They proposed that self-association of asphaltenes is not limited to nanoaggregates but also forms an extended macrostructures in the film with gel-like

rheological properties. As indicated by molecular dynamics simulations, such formation and extension of asphaltene network upon aging were believed to be related to hydrogen bonding interactions mainly induced by sulfoxide groups present in IAA. IAA molecules could form hydrogen bonds with water molecules, resulting in the adsorption at the interface. In addition, hydrogen bonding interactions between neighbouring IAA molecules could provide a pathway for the formation of supramolecular structures.

2.2 Fractionation of asphaltenes based on asphaltene adsorption at oil-solid interface

Despite a great number of chemically distinct compounds acting as the building blocks of asphaltenes, they do not contribute equally to the formation of asphaltene deposits within pipelines and wellbores. Analysis indicated that the asphaltenes extracted from solid deposits contain a higher amount of metals (vanadium, nickel, and iron) and more polar fractions than the asphaltenes separated from parent crudes in the same field.[91] Solid deposit asphaltenes were more prone to form aggregates in toluene compared with their oil counterpart. Heteroatoms (N, O, and S), largely contained in the ring system, have been found to be enriched in asphaltenes adsorbed onto clays in comparison with bulk asphaltenes.[75–77] The adsorption amount of asphaltenes onto kaolinite was reported to increase with increasing nitrogen and sulphur contents of asphaltenes.[77] The presence of heteroatoms in the form of polar functional groups in asphaltenes plays an important role in asphaltene-adsorbent interactions, presumably mainly through hydrogen bonding.[19,63,70] Water, as the most common hydrogen-bonding molecule, can compete with asphaltenes for surface adsorption or even desorb the pre-adsorbed asphaltenes.[63] Less asphaltenes have been found adsorbed onto silica particles after hydrophobic treatment, due to the hindered hydrogen bonding interactions between silanol group on silica surface and polar groups of asphaltenes.[70] In addition, the asphaltenes with a higher degree of aromaticity showed enhanced affinity to adsorbents in both computational[92] and real adsorption studies.[75–77] Although intriguing, it remains unclear as to the correlation between specific structures and adsorption behaviors of asphaltenes. Therefore, it would be informative to fractionate asphaltenes based on their adsorption characteristics to better understand the adsorption mechanisms of asphaltenes at oil-solid interfaces. However, the incomplete

recovery of asphaltenes from the adsorbent limits the application of adsorption-based fractionation. Recently, Sjöblom et al. developed a new fractionation procedure of asphaltenes based on asphaltene adsorption onto calcium carbonate ($CaCO_3$) with a good recovery of 98-99 wt%.[93]

2.2.1 Fractionation procedure

Three different subfractions of asphaltenes were isolated from whole asphaltenes according to their adsorption strengths (Figure 6). The first subfraction, named as bulk asphaltenes, was obtained from the supernatant after centrifugation of mixture of $CaCO_3$ and asphaltene-in-toluene solution. Adsorbed asphaltenes, which are defined as another subfraction of asphaltenes, were then collected from the supernatant following the centrifugation of tetrahydrofuran (THF) and asphaltene-adsorbed $CaCO_3$ obtained from previous step. $CaCO_3$ recovered here was mixed with 50/50 (v/v) THF/$CHCl_3$, followed by the addition of HCl or acetic acid (AA) solution. The organic and aqueous layers were separated subsequently. The last subfraction of asphaltenes, called irreversibly-adsorbed asphaltenes, was extracted from the organic layer. The use of different acids (HCl or acetic acid) had a negligible effect on the composition and structure of irreversibly-adsorbed asphaltenes. Similar elemental analysis results (Table 1) and FTIR spectra were observed for both irreversibly-adsorbed^{HCl} and irreversibly-adsorbed^{AA} asphaltenes. This separation method of asphaltenes is reproducible and quantitative with a recovery of 98-99 wt% of the whole asphaltenes used.

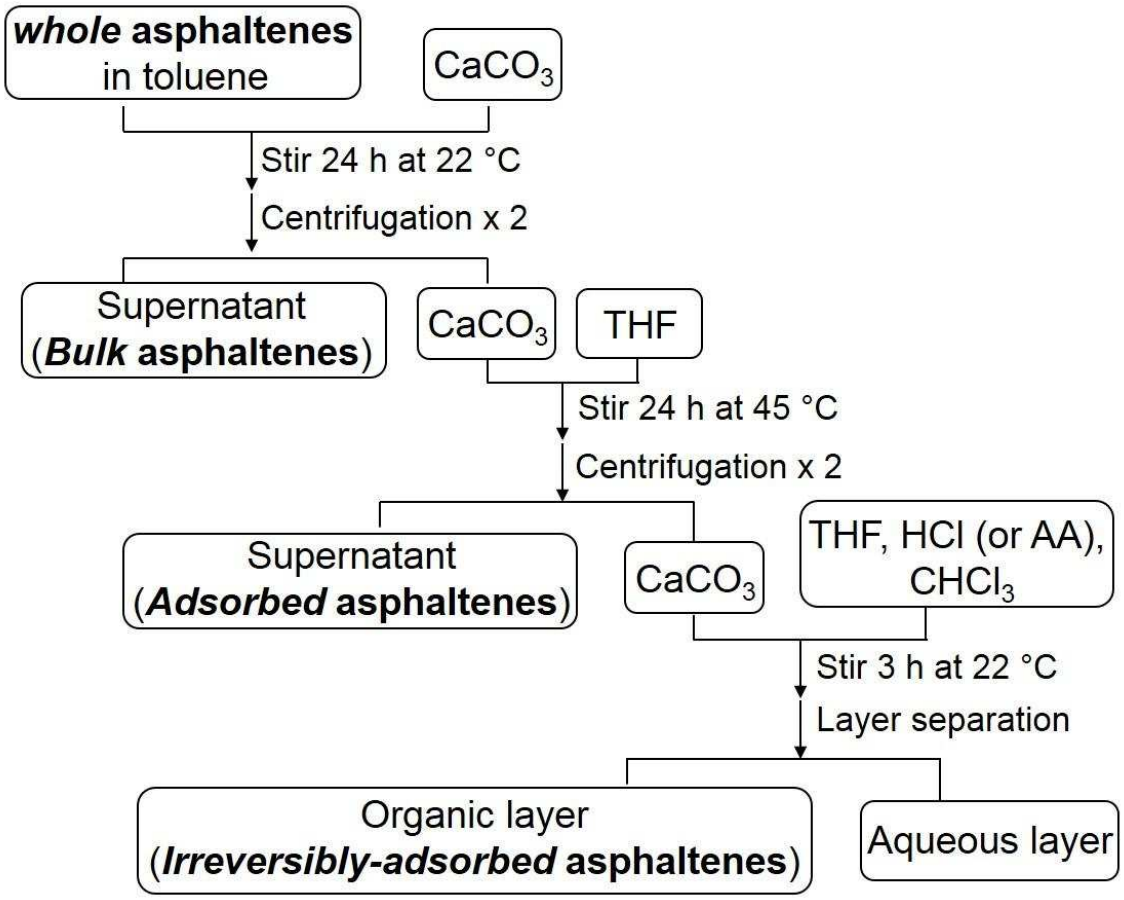

Figure 6. Procedure of asphaltene fractionation based on asphaltene adsorption onto $CaCO_3$. Adapted with permission from Subramanian et al.[93] Copyright 2016 Elsevier.

2.2.2 Chemical compositions

The elemental analysis indicated that all the asphaltene subfractions have similar H/C ratio, nitrogen and sulfur contents (Table 1). As shown in FTIR spectra, they all had resembling absorption peaks in the region of $-CH_3$ and $-CH_2$ stretching vibration (2950 cm^{-1} and 2830 cm^{-1}), suggesting the presence of similar alkyl groups. However, the oxygen content of asphaltene subfractions varied significantly in the range of 2.33 to 4.22 with irreversibly-adsorbed asphaltenes containing the maximum amount of oxygen. Adsorbed asphaltenes have more oxygen than bulk asphaltenes. Such trend was also reflected by FTIR spectra in which irreversibly-adsorbed asphaltenes exhibited the highest adsorption intensity around 1700 cm^{-1}, indicating the highest concentration of carbonyl, carboxylic acid or derivative groups present in them. This adsorption band at 1700 cm^{-1} was found not induced by the contamination of $CaCO_3$. In addition, irreversibly-adsorbed asphaltenes have the lowest

nickel and vanadium contents while the variations are comparatively less between bulk and adsorbed asphaltenes. It should be noted that, compared with whole asphaltenes, the fractionation procedure caused the overall increase of oxygen and calcium due to the oxidation and contamination by $CaCO_3$, as well as the loss of nickel, vanadium and iron resulting from acid treatment and water washing.

Table 1. Elemental analysis of whole asphaltenes and asphaltene subfractions. Adapted with permission from Subramanian et al.[93] Copyright 2016 Elsevier.

Element	*Whole* asphaltenes	Asphaltene subfractions				Mass balance of element (%)
		Bulk	*Adsorbed*	*Irreversibly-adsorbed*^{HCl}	*Irreversibly-adsorbed*^{AA}	
H/C ratio	1.145	1.137	1.139	1.194	1.186	/
N (wt%)	1.32	1.20	1.40	1.35	1.36	-3.0
S (wt%)	1.96	1.91	2.28	2.14	2.13	+4.5
O (wt%)	1.85	2.33	3.27	4.22	3.79	+58.4
Ni (ppm)	77	65	87	40	53	-13
V (ppm)	256	227	266	128	146	-15
Fe (ppm)	96	25	19	<30	<30	-75
Ca (ppm)	1402	6613	3366	655	434	+193

2.2.3 Adsorption properties

Irreversibly-adsorbed asphaltenes showed the ability to form viscoelastic multilayers on the stainless steel surface, while both bulk and adsorbed asphaltenes formed rigid layers on the surface, as detected by QCM-D measurements. The adsorption of all the asphaltene subfractions has also been found quite strong onto the stainless steel surface. In addition, they did not reach the saturation on the surface within the concentration range tested (0.01-1.5 g/L in xylene), unlike whole asphaltenes which exhibited maximum saturation when their concentration was higher than 0.05 g/L in xylene. The highest amount of adsorption

(~8 mg/m^2) was obtained by irreversibly-adsorbed asphaltenes among three asphaltene subfractions with bulk asphaltenes showing the least (~4 mg/m^2), based on the calculated results from Sauerbrey equation. Such adsorption difference could be attributed to the concentration of carboxylic acid groups (irreversibly-adsorbed > adsorbed > bulk), since carboxylic acids tend to interact with chromium (III) oxide on the stainless steel surface thereby inducing the asphaltene adsorption. However, the enhanced adsorption could also result from the diminished interactions between asphaltene subfractions due to the fractionation. This is supported by the fact that the adsorption amount by whole asphaltenes was lower than any of the asphaltene subfractions. Further investigations concerning the interactions between asphaltene subfractions and their detailed structural information are therefore required to clarify the mechanism of asphaltene adsorption on stainless steel.

3. CONCLUSIONS

Asphaltenes are generally recognized as a primary contribution to several major challenges encountered in petroleum processing from the reservoir to the refinery. They are notorious for the stabilization of undesirable W/O emulsions and the formation of solid deposits resulting in fouling and flow-assurance issues. As the oil industry is increasingly turning to unconventional oil resources such as heavy oil, extra heavy oil and oil sands bitumen which contain a large amount of asphaltenes, understanding the role of problematic asphaltenes is of immense scientific and economic importance. Defined as a solubility class by SARA analysis, asphaltenes comprise a broad range of molecules with distinct chemical structures and properties. Considering asphaltenes as a whole was noted to impede the understanding of corresponding mechanisms of asphaltene adsorption at oil-water and oil-solid interfaces. Therefore, E-SARA is proposed as the solution-oriented fractionation of asphaltenes depending on their interfacial activities and adsorption characteristics. Through the determination of active components of asphaltenes, E-SARA enables the identification of key functional groups which participate in asphaltene adsorption. For instance, the stabilization of W/O emulsions by asphaltenes was found mainly due to the IAA subfraction, which accounts less than 2% of whole asphaltenes. The high interfacial activity of IAA molecules, and their ability to produce rigid film with aging effects, were

linked to their high content of sulfoxide groups which could induce the hydrogen bonding interactions between IAA molecules and water as well as neighbouring IAA molecules. In another study concerning the fractionation of asphaltenes based on adsorption onto $CaCO_3$, the whole asphaltenes showed lower adsorption ability onto stainless steel surface than fractionated asphaltenes, in which carbonyl, carboxylic acid or derivative groups play an important role. Thus, E-SARA optimizes the investigation of complex asphaltene systems by distinguishing subfractions of asphaltenes and allowing the correlation of specific functional groups with certain asphaltene characteristics. Under the guidance of the concept of E-SARA fractionation, asphaltene molecules which have critical influences in the relevant systems of interest could be targeted and analyzed. Although the precise chemical structures and molecular associations of active components of asphaltenes remain largely unclear, E-SARA paves the road for future investigation to obtain in-depth understanding of asphaltene behaviors. With the aid of other analytical techniques and computational studies, the exact mechanisms involved are expected to be fully established.

ACKNOWLEDGEMENTS

This research was conducted under the auspices of the Natural Sciences and Engineering Research Council (NSERC)-Industrial Research Chair (IRC) Program in Oil Sands Engineering. The partial support from Alberta Innovates-Energy and Environmental Solutions is also greatly appreciated. The Joint Industrial Program consortium consisting of Norwegian Research Council and oil industry and chemical vendors is gratefully thanked for financial support of the Ugelstad Laboratory group.

REFERENCES

(1) Berkowitz, N. Fossil Hydrocarbons: Chemistry and Technology; Academic Press: San Diego, 1997; pp 83–118.

(2) Bissada, K. K. A.; Tan, J.; Szymczyk, E.; Darnell, M.; Mei, M. Org. Geochem. **2016**, 95, 21–28.

(3) Speight, J. G. Handbook of Petroleum Analysis; Wiley-Interscience: New York, 2001; pp 223–259.

(4) Masliyah, J. H.; Czarnecki, J.; Xu, Z. Handbook on Theory and Practice of Bitumen Recovery from Athabasca Oil Sands; Kingsley Knowledge Publishing: Calgary, 2011; Vol. 1, pp 361–363.

(5) Jewell, D. M.; Weber, J. H.; Bunger, J. W.; Plancher, H.; Latham, D. R. Anal. Chem. **1972**, 44, 1391–1395.

(6) Jewell, D. M.; Albaugh, E. W.; Davis, B. E.; Ruberto, R. G. Ind. Eng. Chem. Fundam. **1974**, 13, 278–282.

(7) Sheu, E. Y. Energy Fuels **2002**, 16, 74–82.

(8) Santos, R. G.; Loh, W.; Bannwart, A. C.; Trevisan, O. V. Braz. J. Chem. Eng. **2014**, 31, 571–590.

(9) Nikookar, M.; Omidkhah, M. R.; Pazuki, G. R. Pet. Sci. Technol. **2008**, 26, 1904–1912.

(10) Cho, Y.; Kim, Y. H.; Kim, S. Anal. Chem. **2011**, 83, 6068–6073.

(11) Cho, Y.; Na, J.-G.; Nho, N.-S.; Kim, S.; Kim, S. Energy Fuels **2012**, 26, 2558–2565.

(12) Langevin, D.; Argillier, J.-F. Adv. Colloid Interface Sci. **2016**, 233, 83–93.

(13) Fan, T.; Buckley, J. S. Energy Fuels **2002**, 16, 1571–1575.

(14) Kharrat, A. M.; Zacharia, J.; Cherian, V. J.; Anyatonwu, A. Energy Fuels **2007**, 21, 3618–3621.

(15) Akbarzadeh, K.; Hammami, A.; Kharrat, A.; Zhang, D.; Allenson, S.; Creek, J.; Kabir, S.; Jamaluddin, A. J.; Marshall, A. G.; Rodgers, R. P.; Mullins, O. C.; Solbakken, T. Oilfield. Rev. **2007**, 19, 22–43.

(16) Drummond, C.; Israelachvili, J. J. Pet. Sci. Eng. **2004**, 45, 61–81.

(17) Vafaie-Sefti, M.; Mousavi-Dehghani, S. A. Fluid Phase Equilib. **2006**, 247, 182–189.

(18) Syunyaev, R. Z.; Balabin, R. M.; Akhatov, I. S.; Safieva, J. O. Energy Fuels **2009**, 23, 1230–1236.

(19) Adams, J. J. Energy Fuels **2014**, 28, 2831–2856.

(20) Torres, C. A.; Treint, F.; Alonso, C.; Milne, A.; Lecomte, A. SPE/ICoTA Coiled Tubing Conference and Exhibition; The Woodlands, TX, April 12−13, 2005; SPE 93272.

(21) McLean, J. D.; Kilpatrick, P. K. J. Colloid Interface Sci. **1997**, 196, 23–34.

(22) Yan, Z.; Elliott, J. A. W.; Masliyah, J. H. J. Colloid Interface Sci. **1999**, 220, 329–337.

(23) Yarranton, H. W.; Hussein, H.; Masliyah, J. H. J. Colloid Interface Sci. **2000**, 228, 52–63.

(24) Gafonova, O. V.; Yarranton, H. W. J. Colloid Interface Sci. **2001**, 241, 469–478.

(25) Spiecker, P. M.; Gawrys, K. L.; Kilpatrick, P. K. J. Colloid Interface Sci. **2003**, 267, 178–193.

(26) Kilpatrick, P. K. Energy Fuels **2012**, 26, 4017–4026.

(27) Gawel, I.; Bociarska, D.; Biskupski, P. Appl. Catal., A **2005**, 295, 89–94.

(28) Marchal, C.; Abdessalem, E.; Tayakout-Fayolle, M.; Uzio, D. Energy Fuels **2010**, 24, 4290–4300.

(29) Mullins, O. C.; Martínez-Haya, B.; Marshall, A. G. Energy Fuels **2008**, 22, 1765–1773.

(30) Mullins, O. C. Annu. Rev. Anal. Chem. **2011**, 4, 393–418.

(31) Schuler, B.; Meyer, G.; Peña, D.; Mullins, O. C.; Gross, L. J. Am. Chem. Soc. **2015**, 137, 9870–9876.

(32) Merino-Garcia, D.; Andersen, S. I. Pet. Sci. Technol. **2003**, 21, 507–525.

(33) Yarranton, H. W. J. Dispers. Sci. Technol. **2005**, 26, 5–8.

(34) Wang, S.; Liu, J.; Zhang, L.; Masliyah, J.; Xu, Z. Langmuir **2010**, 26, 183–190.

(35) Zhang, L.; Shi, C.; Lu, Q.; Liu, Q.; Zeng, H. Langmuir **2016**, 32, 4886–4895.

(36) Dickie, J. P.; Yen, T. F. Anal. Chem. **1967**, 39, 1847–1852.

(37) Mullins, O. C. Energy Fuels **2010**, 24, 2179–2207.

(38) Mullins, O. C.; Sabbah, H.; Eyssautier, J.; Pomerantz, A. E.; Barré, L.; Andrews, A. B.; Ruiz-Morales, Y.; Mostowfi, F.; McFarlane, R.; Goual, L.; Lepkowicz, R.; Cooper, T.; Orbulescu, J.; Leblanc, R. M.; Edwards, J.; Zare, R. N. Energy Fuels **2012**, 26, 3986–4003.

(39) Rodgers, R. P.; Marshall, A. G. In Asphaltenes, Heavy Oils and Petroleomics; Mullins, O. C., Sheu, E. Y., Hammami, A., Marshall, A. G., Eds.; Springer: New York, 2007; pp 63-93.

(40) Pinkston, D. S.; Duan, P.; Gallardo, V. A.; Habicht, S. C.; Tan, X.; Qian, K.; Gray, M.; Mullen, K.; Kenttämaa, H. I. Energy Fuels **2009**, 23, 5564–5570.

(41) Borton, D.; Pinkston, D. S.; Hurt, M. R.; Tan, X.; Azyat, K.; Tywinsky, R.; Gray, M.; Qian, K.; Kenttämaa, H. I. Energy Fuels **2010**, 24, 5548−5559.

(42) Gray, M. R.; Tykwinski, R. R.; Stryker, M.; Tan, X. Energy Fuels **2011**, 25, 3125–3134.

(43) Sedghi, M.; Goual, L.; Welch, W.; Kubelka, J. J. Phys. Chem. B **2013**, 117, 5765–5776.

(44) Mikami, Y.; Liang, Y.; Matsuoka, T.; Boek, E. S. Energy Fuels **2013**, 27, 1838–1845.

(45) Gao, F.; Xu, Z.; Liu, G.; Yuan, S. Energy Fuels **2014**, 28, 7368–7376.

(46) Liu, J.; Zhao, Y.; Ren, S. Energy Fuels **2015**, 29, 1233–1242.

(47) Yeung, A.; Dabros, T.; Masliyah, J.; Czarnecki, J. Colloids Surf., A. **2000**, 174, 169–181.

(48) Gao, S.; Moran, K.; Xu, Z.; Masliyah, J. Energy Fuels **2009**, 23, 2606–2612.

(49) Freer, E. M.; Radke, C. J. J. Adhes. **2004**, 80, 481–496.

(50) Yarranton, H. W.; Sztukowski, D. M.; Urrutia, P. J. Colloid Interface Sci. **2007**, 310, 246–252.

(51) Harbottle, D.; Chen, Q.; Moorthy, K.; Wang, L.; Xu, S.; Liu, Q.; Sjoblom, J.; Xu, Z. Langmuir **2014**, 30, 6730–6738.

(52) Sztukowski, D. M.; Yarranton, H. W. Langmuir **2005**, 21, 11651–11658.

(53) Quintero, C. G.; Noïk, C.; Dalmazzone, C.; Grossiord, J. L. Oil Gas Sci. Technol. **2009**, 64, 607–616.

(54) Verruto, V. J.; Le, R. K.; Kilpatrick, P. K. J. Phys. Chem. B **2009**, 113, 13788–13799.

(55) Alvarez, G.; Poteau, S.; Argillier, J.-F.; Langevin, D.; Salager, J.-L. Energy Fuels **2009**, 23, 294–299.

(56) Rane, J. P.; Pauchard, V.; Couzis, A.; Banerjee, S. Langmuir **2013**, 29, 4750–4759.

(57) Spiecker, P. M.; Kilpatrick, P. K. Langmuir **2004**, 20, 4022–4032.

(58) Tchoukov, P.; Yang, F.; Xu, Z.; Dabros, T.; Czarnecki, J.; Sjöblom, J. Langmuir **2014**, 30, 3024–3033.

(59) Harbottle, D.; Liang, C.; El-thaher, N.; Liu, Q.; Masliyah, J.; Xu, Z. Particle-Stabilized Emulsions and Colloids, 2015, 283-316.

(60) Zahabi, A.; Gray, M. R.; Dabros, T. Energy Fuels **2012**, 26, 1009–1018.

(61) Dudášová, D.; Silset, A.; Sjöblom, J. J. Dispers. Sci. Technol. **2008**, 29, 139–146.

(62) González, M. F.; Stull, C. S.; López-Linares, F.; Pereira-Almao, P. Energy Fuels

2007, 21, 234–241.

(63) Carbognani, L. Pet. Sci. Technol. **2000**, 18, 335–360.

(64) Ekholm, P.; Blomberg, E.; Claesson, P.; Auflem, I. H.; Sjöblom, J.; Kornfeldt, A. J. Colloid Interface Sci. **2002**, 247, 342–350.

(65) Rudrake, A.; Karan, K.; Horton, J. H. J. Colloid Interface Sci. **2009**, 332, 22–31.

(66) Xie, K.; Karan, K. Energy Fuels **2005**, 19, 1252–1260.

(67) Goual, L.; Abudu, A. Energy Fuels **2010**, 24, 469–474.

(68) Acevedo, S.; Castillo, J.; Fernández, A.; Goncalves, S.; Ranaudo, M. A. Energy Fuels **1998**, 12, 386–390.

(69) Clementz, D. M. Clays Clay Miner. **1976**, 24, 312–319.

(70) Dudášová, D.; Simon, S.; Hemmingsen, P. V.; Sjöblom, J. Colloids Surf., A. **2008**, 317, 1–9.

(71) Jada, A.; Debih, H.; Khodja, M. J. Pet. Sci. Eng. **2006**, 52, 305–316.

(72) Jada, A.; Debih, H. Compos. Interfaces **2009**, 16, 219–235.

(73) Klein, G. C.; Kim, S.; Rodgers, R. P.; Marshall, A. G.; Yen, A. Energy Fuels **2006**, 20, 1973–1979.

(74) Pernyeszi, T.; Patzkó, Á.; Berkesi, O.; Dékány, I. Colloids Surf., A. **1998**, 137, 373–384.

(75) Tu, Y.; Kung, J.; McCracken, T.; Kotlyar, L.; Kingston, D.; Sparks, B. Clay Sci. **2006**, 12, 194–198.

(76) Tu, Y.; Woods, J.; Kung, J.; McCracken, T.; Kotlyar, L.; Sparks, B.; Dong, M. Clay Sci. **2006**, 12, 183–187.

(77) Tu, Y.; Woods, J.; McCracken, T.; Kotlyar, L.; Sparks, B.; Chung, K. Clay Sci. **2006**, 12, 188–193.

(78) Czarnecka, E.; Gillott, J. E. Clays Clay Miner. **1980**, 28, 197–203.

(79) Hannisdal, A.; Ese, M.-H.; Hemmingsen, P. V.; Sjöblom, J. Colloids Surf., A. **2006**, 276, 45–58.

(80) Xu, Y.; Dabros, T.; Hamza, H.; Shefantook, W. Pet. Sci. Technol. **1999**, 17, 1051–1070.

(81) Wu, X. Energy Fuels **2003**, 17, 179–190.

(82) Stanford, L. A.; Rodgers, R. P.; Marshall, A. G.; Czarnecki, J.; Wu, X. A.; Taylor, S. Energy Fuels **2007**, 21, 973–981.

(83) Czarnecki, J.; Tchoukov, P.; Dabros, T. Energy Fuels **2012**, 26, 5782–5786.

(84) Czarnecki, J.; Tchoukov, P.; Dabros, T.; Xu, Z. Can. J. Chem. Eng. **2013**, 91, 1365–1371.

(85) Yang, F.; Tchoukov, P.; Pensini, E.; Dabros, T.; Czarnecki, J.; Masliyah, J.; Xu, Z. Energy Fuels **2014**, 28, 6897–6904.

(86) Yang, F.; Tchoukov, P.; Dettman, H.; Teklebrhan, R. B.; Liu, L.; Dabros, T.; Czarnecki, J.; Masliyah, J.; Xu, Z. Energy Fuels **2015**, 29, 4783−4794.

(87) Fossen, M.; Kallevik, H.; Knudsen, K. D.; Sjöblom, J. Energy Fuels **2007**, 21, 1030–1037.

(88) Kharrat, A. M. Energy Fuels **2009**, 23, 828–834.

(89) Jarvis, J. M.; Robbins, W. K.; Corilo, Y. E.; Rodgers, R. P. Energy Fuels **2015**, 29, 7058–7064.

(90) Japanwala, S.; Chung, K. H.; Dettman, H. D.; Gray, M. R. Energy Fuels **2002**, 16, 477–484.

(91) Wattana, P., Fogler, H. S., Yen, A., Carmen Garcia, M. D. and Carbognani, L. Energy Fuels **2005**, 19, 101–110.

(92) Alvarez-Ramírez, F.; García-Cruz, I.; Tavizón, G.; Martínez-Magadán, J. M. Pet. Sci. Technol. **2004**, 22, 915–926.

(93) Subramanian, S.; Simon, S.; Gao, B.; Sjöblom, J. Colloids Surf., A. **2016**, 495, 136–

148.